Journal of Biomedical Optics

SPIEDigitalLibrary.org/jbo

Optical coherence tomography provides an ability to assess mechanical property of cardiac wall of developing outflow tract in embryonic heart *in vivo*

Peng Li
Ruikang K. Wang

SPIE

Optical coherence tomography provides an ability to assess mechanical property of cardiac wall of developing outflow tract in embryonic heart *in vivo*

Peng Li and Ruikang K. Wang
University of Washington, Department of Bioengineering, 3720 15th Avenue Northeast, Seattle, Washington 98195

Abstract. Knowledge of the biomechanical/elastic property of the cardiac wall is of fundamental importance in improving our understanding of cardiac development, particularly the interaction between the wall dynamics and hemodynamics in the developing outflow tract (OFT). We describe a method that employs optical coherence tomography (OCT) as a means to noninvasively measure the local elastic property of the cardiac wall *in vivo*. The method uses a time-lapse sequence of OCT images that represent the dynamic behavior of the OFT longitudinal section to calculate the regional wall pulse wave velocity (PWV), upon which the Young's modulus of the cardiac wall is deduced by the use of the Moens-Korteweg equation. The experimental results show that the foot-to-foot PWV ranges from 3.2 to 6.6 mm/s with a mean of 4.7 mm/s, and the averaged Young's modulus is 0.36 Pa, both of which are comparable to the documented values of stage HH17 atrioventricular canal tissue. The proposed method that provides the quantitative mechanical assessment may play a significant role in the understanding of the cardiac development. [DOI: 10.1117/1.JBO.17.12.120502]

Keywords: optical coherence tomography; medical and biological imaging; cardiac development; wall pulse wave velocity; wall elastic property; embryonic chick heart.

Paper 12658L received Oct. 2, 2012; revised manuscript received Nov. 1, 2012; accepted for publication Nov. 8, 2012; published online Dec. 3, 2012.

Progressive alternation of biomechanical/elastic property and tissue composition of the cardiac wall is closely associated with the cardiac development in the developing embryonic heart.[1] There is substantial evidence[2] suggesting that intrinsic genetic expression is regulated by the local biomechanical environment that is determined by the dynamic interaction between the cardiac wall and flowing blood. To understand the cardiac development, particularly the interaction between wall dynamics and hemodynamics in developing outflow tract (OFT, a distal heart portion that connects the ventricle to the arterial system), a knowledge of the biomechanical/elastic properties of the cardiac wall is of fundamental importance.

Pulse wave velocity (PWV) of the cardiac wall is highly correlated with the elastic properties.[3] The wall PWV may be used to determine the Young's modulus of the cardiac wall. There is no technique currently available that is capable of measuring the mechanical properties of the cardiac wall *in vivo*, without harm to the developing heart. Optical coherence tomography (OCT) is capable of noninvasive, noncontact, volumetric imaging of turbid tissue with high temporal (~μs range) and spatial (~μm) resolution.[4,5] In this letter, we propose to use the time-lapse sequence of OCT images that is captured at the OFT longitudinal section by an ultrafast OCT system to calculate the wall PWV, from which the elasticity of the OFT wall is deduced. To demonstrate the proof of the concept, we used the stage HH18 chick embryos as the animal model in this study.

The chick embryo preparation and the OCT system setup has been elucidated in Ref. 6. To increase the imaging speed and the image definition, and to enhance the ability of capturing fast events of the embryonic beating heart, a dual-camera spectral domain optical coherence tomography (SD-OCT) configuration was used that operated at 1310 nm wavelength region, providing a ~184 KHz A-line scan rate and ~10 μm spatial resolution.[6] In order to quantify the longitudinal propagation of the wall pulse wave along the OFT wall, 1000 repeated B-frames (a time sequence of OFT longitudinal sections, $z + x + t$) were acquired at an imaging rate of ~280 frames per second (fps), covering ~8 cardiac cycles of the beating heart.

The schematic of measuring the wall PWV is illustrated in Fig. 1. Along the OFT longitudinal section, we selected a number of radial lines that are almost perpendicular to the OFT wall (marked by the red lines a to g) with a known distance between each line as measured from the OCT images. After selecting these radial lines, the M-mode structure images (time lapse profiles along the marked lines) were then digitally extracted from the available three-dimensional (3-D) time-lapse longitudinal volumetric OCT images (refer to Figs. 2 and 3), from which the pulse wave of the myocardial wall motion was computed. From the pulse waves, the regional foot-to-foot wave velocity (V_{ff}) was readily available by calculating the time delay (t_{ff}) between the initial opening and the ultimate closing of the myocardial wall between a known distance (L) apart [refer to Fig. 3(c)][7]:

$$V_{\mathrm{ff}} = \frac{L}{t_{\mathrm{ff}}}. \tag{1}$$

And the regional apparent phase velocity (V_{app}) was calculated using the apparent time delay (t_{app}), which can be measured by differentiating the phases of corresponding fundamental harmonics ($\Delta\theta$) at the two locations[7,8]:

$$t_{\mathrm{app}} = \frac{\Delta\theta}{(2\pi f)'}. \tag{2}$$

where f is the heart rate.

For a transverse wave on a viscoelastic conduit with a relatively small wall thickness (compared to its diameter) filled with an incompressible fluid, a simple model of the well-known Moens-Korteweg equation can be used to describe the relationship between the wave propagation and the elasticity

Address all correspondence to: Ruikang K. Wang, University of Washington, Department of Bioengineering, 3720 15th Avenue Northeast, Seattle, Washington 98195. Tel: 206 6165025; Fax: 206 6853300; E-mail: wangrk@uw.edu

0091-3286/2012/$25.00 © 2012 SPIE

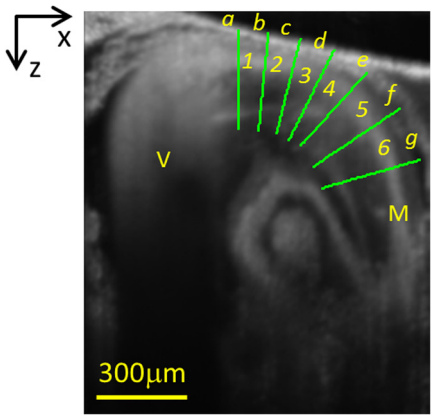

Fig. 1 OCT image of the longitudinal section of the OFT averaged over ~7 cardiac cycles, sketching the measurement of the PWV. Red lines (a–g) indicate the sites for extracting pulsatile motion of myocardial wall. Six segments in total are used for PWV measurement of myocardial wall in this case. V: ventricle; M: myocardium.

property.[9,10] Thus, the Young's modulus (E) of the myocardial wall could be derived from the measured wall PWV (V):

$$E = \frac{2R\rho V^2}{h}, \tag{3}$$

where h is the wall thickness, ρ is the density of the wall (similar to the blood) and R is the radius of the OFT.

As shown in Fig. 2, the simultaneous M-mode images of the instantaneous myocardial wall motion were extracted from the time sequence of OFT longitudinal sections along the lines [Fig. 2(a) to 2(g)], respectively. These figures represent seven descending OFT positions marked as "a" to "g" in Fig. 1. Based on the image segmentation,[11] the instantaneous positions of the myocardial wall boundary were obtained from the M-mode images as depicted by the curves in Fig. 2. Accordingly, the pulse waves of the wall motion were obtained at the seven descending OFT positions as shown in Fig. 3(a). The corresponding fundamental harmonic waves of the wall motion are plotted in Fig. 3(b).

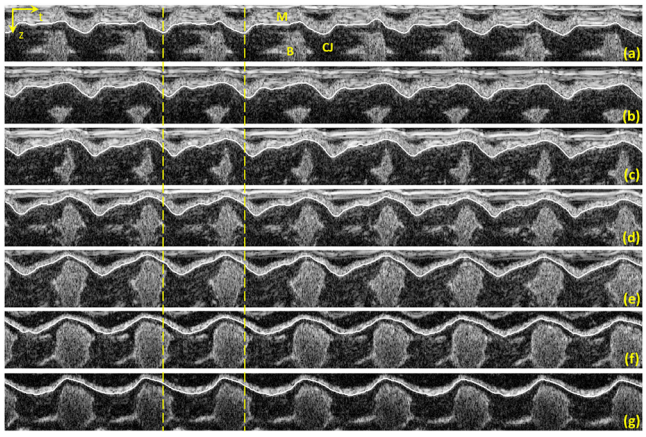

Fig. 2 Simultaneous M-mode images of the instantaneous myocardial wall motion along the lines (a-g), respectively, distributed at seven descending OFT positions marked in Fig. 1. Solid lines depict the inner boundary of the myocardial wall. Dashed lines indicate one cardiac cycle in (a). M: myocardium; CJ: cardiac jelly; B: blood.

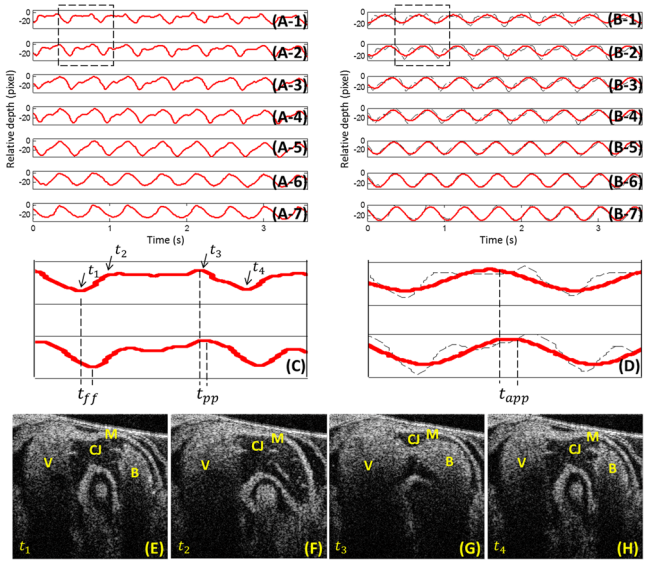

Fig. 3 Pulse wave of the myocardial wall simultaneously obtained throughout OFT as extracted from the available 3-D volumetric time-lapse longitudinal dataset. (A, B), Pulse waves and fundamental harmonics of myocardial wall, respectively, corresponding to the positions of a–g in Figs. 1 and 2. (C, D) enlarged view of the wall pulse waveforms as marked in (A) and (B), respectively. (E-F) Typical OCT images represent the longitudinal sections of OFT corresponding to the time instants at V: ventricle; M: myocardium; CJ: cardiac jelly; B: blood.

Figure 3(c) shows an enlarged view of a typical waveform of the myocardial wall motion. The arrows t_1 and t_4 in Fig. 3(c), respectively correspond to the longitudinal sections in Fig. 3(e) and 3(h), indicating the instantaneous times of the initial opening and the ultimate closing of the myocardial wall when the OFT is most contracted. The principal peak as marked by the arrow t_3 in Fig. 3(c) corresponds to the longitudinal section in Fig. 3(g), being the instant of blood ejection from the ventricle when the OFT is most expanded and filled with blood. It is interesting to note that there exists a secondary peak as marked by the arrow t_2 in Fig. 3(c). Such a secondary peak is apparent for the positions of "a" to "d" in Figs. 1 and 2 where the outflow cushion (OC) was present. This secondary peak is most likely due to the OC expansion, which has been reported to happen prior to the ventricle ejection for the stage HH18 chick embryos.[6,12]

Due to the high spatial resolution of OCT, the distance between each position was precisely calculated [Fig. 4(a)]. The corresponding time delays (both foot-to-foot t_{ff} and apparent t_{app}) are plotted in Fig. 4(b) as a function of the locations. Consequently, both the foot-to-foot PWV V_{ff} and the apparent PWV V_{app} can be made readily available [Fig. 4(c)].

From Fig. 4, the mean foot-to-foot PWV was evaluated to be 4.7 mm/s for the chick embryo we used in this study. The ratio of the OFT radius to the wall thickness R/h was estimated to be 7.66 from the OCT M-mode images and the blood density was assumed to be 1060 kg/m^3. Based on these values, the Young's modulus of the myocardial wall $E = 0.36$ Pa was then deduced from Eq. (3).

In this letter, a method based on dynamic structure tracking has been developed to quantify the elastic properties of the myocardial wall, including PWV and Young's modulus. In the study, it was assumed that the wall pulse wave from the seven positions in Fig. 1 was measured simultaneously. However, the OCT longitudinal section was acquired line by line (A scan-by-A scan).

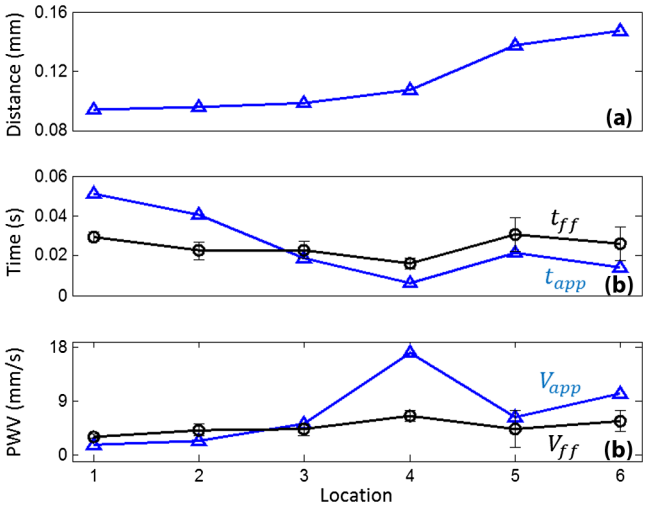

Fig. 4 Plots of the distance (A), time delay (B) and PWV (C) as a function of the descending locations in OFT.

The maximal lateral spatial interval in the six wall regions in Fig. 1 is ~40 pixels, thus there exists a maximal ~0.2 ms inherent time delay t_0 between each pulse wave, as shown in Fig. 3(a). Fortunately, the minimal foot-to-foot time delay is $t_{\text{ff min}} = 16.3$ ms and the minimal apparent time delay is $t_{\text{app min}} = 6.3$ ms [refer to Fig. 4(b)]. Accordingly, the inherent time delay t_0 due to the line-by-line imaging nature of the OCT system is relatively too small to account for noticeable errors in the evaluations.

Comparing the foot-to-foot velocity V_{ff} and the apparent velocity V_{app} for each wall segments, a significant difference exists at the location 4 [refer to Fig. 4(c)]. Such difference between the foot-to-foot velocity and the apparent velocity is very similar to the situation of the blood pulse wave propagating in the human aortic region at the level of the renal arteries, where the strong local reflection due to the renal branch was well documented to influence the apparent velocity.[7] Thus, the significant difference in OFT at location 4 could be ascribed to the influence of the bend of the wall at this location.

According to Eq. (3), for viscoelastic conduits with the same elastic property E, the smaller radius R would correspond to the higher pulse velocity V. Referring to Fig. 1, from locations 1 to 6, the OFT radius gradually decreases, while the wall foot-to-foot velocity gradually increases [Fig. 4(c)]. This observation is in good agreement with a prior study where the foot-to-foot velocity along the descending human aorta reported in Fig. 5 of Ref. 7 was increased with the decrease of the aorta radius.

The measured foot-to-foot PWV ranged from 3.2 to 6.6 mm/s with a mean of 4.7 mm/s, and the averaged Young's modulus was calculated to be 0.36 Pa. Due to the lack of corresponding OFT value in the literature, the tissue wave propagation in atrioventricular (AV) canals of HH17 and HH24 embryonic chick was taken for comparison. According to Ref. 1, in the AV canals of HH17 and HH24 embryonic chick, the tissue wave speed was approximately 8 mm/s and 6 mm/s, and the effective modulus was 0.15 and 0.85 Pa, respectively. Generally, our measurement was on the same scale as that reported in Ref. 1. The discrepancy was most likely due to the different embryonic stages, different tissue, and different measuring methods used.

In this study, the wall PWV measurement is based on the dynamic structure tracking. Although this method served well for the purpose of proof-of-concept demonstration, the accuracy of pulse wave evaluation, particularly the high frequency components, is highly dependent upon the accuracy of image segmentation. Further improvement can be realized by measuring the pulsatile strain rate of the myocardial wall (based on the Doppler method) for timing the propagation of the wall pulse wave.[6] Beside the cardiac development, possible applications of the wall PWV may also be found in the intravascular OCT for characterizing the elastic property of arterial wall.

References

1. J. T. Butcher et al., "Transitions in early embryonic atrioventricular valvular function correspond with changes in cushion biomechanics that are predictable by tissue composition," *Circ. Res.* **100**(5), 1503–1511 (2007).
2. J. R. Hove et al., "Intracardiac fluid forces are an essential epigenetic factor for embryonic cardiogenesis," *Nature* **421**(6919), 172–177 (2003).
3. W. W. Nichols, M. F. O'Rourke, and C. Vlachopoulos, *McDonald's Blood Flow in Arteries: Theoretical, Experimental and Clinical Principles*, 6th ed., Hodder Arnold, London (2011).
4. A. F. Fercher et al., "Optical coherence tomography—principles and applications," *Rep. Prog. Phys.* **66**(1), 239–303 (2003).
5. P. H. Tomolins and R. K. Wang, "Theory, developments and applications of optical coherence tomography," *J. Phys. D: Appl. Phys.* **38**(7), 2519–2535 (2005).
6. P. Li et al., "*In vivo* functional imaging of blood flow and wall strain rate in outflow tract of embryonic chick heart using ultrafast spectral domain optical coherence tomography," *J. Biomed. Opt.* **17**(9), 096006 (2012).
7. R. D. Latham et al., "Regional wave travel and reflections along the human aorta: a study with six simultaneous micromanometric pressures," *Circulation* **72**(6), 1257–1269 (1985).
8. S. Solomon et al., "Determination of vascular impedance in the peripheral circulation by transcutaneous pulsed Doppler ultrasound," *Chest* **108**(2), 515–521 (1995).
9. M. Pernot et al., "ECG-gated, mechanical and electromechanical wave imaging of cardiovascular tissues *in vivo*," *Ultrasound Med. Biol.* **33**(7), 1075–1085 (2007).
10. D. J. Korteweg, "Ueber die Fortpflanzungsgeschwindigkeit des Schalles in elastischen Röhren," *Annalen der Physik* **241**(12), 525–542 (1878).
11. X. Yin et al., "Extracting cardiac shapes and motion of the chick embryo heart outflow tract from four-dimensional optical coherence tomography images," *J. Biomed. Opt.* **17**(9), 096005 (2012).
12. A. M. Oosterbaan et al., "Doppler flow velocity waveforms in the embryonic chicken heart at developmental stages corresponding to 5–8 weeks of human gestation," *Ultrasound in Obstet. Gynecol.* **33**(6), 638–644 (2009).